

Employment of Silicon Nitride Films Prepared by DC Reactive Sputtering Technique for Ion Release Applications

Diyar A. Taher^{1a*} and Mohammed A. Hameed^{1b}

¹Department of Physics, College of Science, University of Baghdad, Baghdad, Iraq

^bE-mail: mohammedabdullah197575@gmail.com

^{a*}Corresponding author: diyarali176@gmail.com

Abstract

In this work, silicon nitride (Si_3N_4) thin films were deposited on metallic substrates (aluminium and titanium sheets) by the DC reactive sputtering technique using two different silicon targets (n-type and p-type Si wafers) as well as two $\text{Ar}:\text{N}_2$ gas mixing ratios (50:50 and 70:30). The electrical conductivity of the metallic (aluminium and titanium) substrates was measured before and after the deposition of silicon nitride thin films on both surfaces of the substrates. The results obtained from this work showed that the deposited films, in general, reduced the electrical conductivity of the substrates, and the thin films prepared from n-type silicon targets using a 50:50 mixing ratio and deposited on both surfaces of a titanium substrate reduced the electrical conductivity of this substrate by 30%. This reduction in the release of ions from the coated metal substrate is attributed to the dielectric properties of the deposited silicon nitride thin films. This result is very important and applicable. This work represents the first attempt in Iraq to study such effects and may represent a good starting point for advanced studies in biomedical engineering.

Article Info.

Keywords:

Biomedical applications, DC Reactive Sputtering Technique, Electrical conductivity, Ion release, Silicon nitride.

Article history:

Received: Jun.07,2023

Revised: Aug. 07, 2023

Accepted: Aug.12,2023

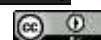
Published: Sep.01,2023

1. Introduction

Silicon nitride (Si_3N_4) is characterized by its high chemical stability, high strength, very low thermal expansion coefficient, large energy gap (up to 5.3 eV), high dielectric constant (~ 7), and very high electrical resistivity ($\sim 10^{13} \Omega\cdot\text{cm}$) [1-3]. These characteristics made it one of the most important ceramic materials used as an insulating material in the manufacture of passive and active electronic and electro-optic devices as well as nonlinear optics that operate at high temperatures and harsh conditions, such as gas sensors in nuclear power plants, space stations and spacecraft [1, 3, 4]. Si_3N_4 is a hard optical material which with good piezoelectric response [5, 6]. Aside from their many optical applications, Si_3N_4 thin films offer surface passivation applications for microcrystalline silicon solar cell [7], piezoelectric transducers with high frequencies, biomedical applications [8, 9], and nanocomposites [10, 11].

In biomedical applications, metals, such as silicon nitride, are used for joint replacements, dental bridges and implants, and coronary stents. The presence of such metals and their continuous release may cause lasting harmful effects in tissues due to their inability to biodegrade. Also, the additional exposure to the electric fields may shorten the time required for cellular healing [12]. Metal toxicity is influenced by several parameters, making it difficult to accurately determine the quantities that cause cellular harm. The corrosion of an alloy is critical to its biocompatibility since elemental release from the alloy almost always causes unfavourable biologic consequences such as toxicity, allergies, mutagenicity, and carcinogenicity [13]. Alloy corrosion releases free ions into the surrounding tissues. There is minimal evidence that components produced by casting alloys contribute significantly to systemic toxicity. This could be explained by the slow release of ions over time [14].

Si_3N_4 is the most effective material for covering the *in vivo* parts made of metal and metallic alloys to prevent the release of metallic ions into the living body.



Therefore, the electrical properties of Si_3N_4 used in biomedical applications are of extraordinary importance [1, 15].

Over many decades, Si_3N_4 powders and thin films with different phases have been prepared using different methods and techniques, including chemical and physical, such as ion-assisted deposition [16, 17], heating powdered silicon [18, 19], carbothermal reduction [20-22], chemical vapor deposition (CVD) [23-27], plasma-enhanced CVD [28], nitrogen glow discharge [29, 30], atomic layer deposition (ALD) [31-33], silane-ammonia reaction [34], and reactive sputtering [35-43]. However, the effect of the electrical conductivity of silicon used as a precursor of silicon nitride was not determined. The electrical characteristics of Si_3N_4 as a biomaterial are very important and should be accurately studied.

Obviously, electrical properties of compound materials, such as Si_3N_4 , are mainly determined by their structural characteristics, which are dependent on the preparation or synthesis method. The SiN_4 tetrahedron is the fundamental unit of Si_3N_4 , having a silicon atom at the center and four nitrogen atoms at each corner. Sharing corners connect the SiN_4 tetrahedra, ensuring every atom of nitrogen is divided by three tetrahedra. As a result, nitrogen is surrounded by three silicon atoms [44]. The structural difference between α - Si_3N_4 and β - Si_3N_4 can be explained by different arrangements of Si-N layers. The fundamental units are connected to produce wrinkled or puckered six-membered rings that encircle enormous holes. These basal planes serve as the foundation for α Si_3N_4 and β Si_3N_4 structures [45]. The bulk silicon as a wafer or powder is the most prevalent source of silicon atoms in atomic scale preparation methods and procedures. As a result, the electrical conductivity of this source may be essential in defining the electrical characteristics of the produced silicon nitride [46].

The aim of the work is to study the effect of the type of electrical conductivity of silicon wafers used as targets for DC reactive sputtering on the electrical conductivity of Si_3N_4 thin films deposited on metallic substrates.

The DC reactive magnetron sputtering technique was chosen for the preparation of Si_3N_4 thin films because of its many advantages over the other thin film deposition methods and techniques. The most important advantages are preparation of high-quality defect-free films, high deposition rate, and easy control of elemental composition and structure of the growing film. Such advantages make this technique most widely used to prepare optical coatings, hard coatings for cutting tools, decorative coatings, microelectronics, optoelectronics and solar cells [3, 5, 10, 38-43].

2. Experimental Work

Si_3N_4 thin films were deposited on metallic substrates (aluminium and titanium) using DC reactive magnetron sputtering technique. In this technique, gas mixtures of argon and nitrogen with two different mixing ratios (50:50 and 70:30) were used. Two silicon targets with different types of conductivity (n-type and p-type) were used. The deposition chamber was initially evacuated down to 0.001 torr. Deposition process was carried out at room temperature using gas mixture pressure of 0.8 torr, discharge voltage of 730V, and discharge current of 50 mA. Deposition time was 4 hours for all samples. More details on the optimum preparation conditions can be found elsewhere [35-41].

Fig. 1 shows the DC reactive sputtering system used in this work. It contains a deposition chamber made of stainless steel with eight windows to monitor what is happening inside it. The anode and cathode of the discharge system are fixed inside this chamber, with holders outside the chamber to be connected to the DC power supply. The chamber also contains the inlet of the gas mixture from an outer mixer. The chamber is evacuated through an outlet connected to the rotary pump. The applied and discharge voltages are continuously measured by voltmeters, while the discharge

current is measured by an ammeter connected between the anode and cathode. The flow rate of the gas mixture into the deposition chamber can be precisely controlled, and the temperature inside the chamber is measured by a precise thermometer. The gas mixer is supplied with argon and nitrogen gases from gas cylinders and the mixing ratio is controlled by accurate needle valves. Both the anode and cathode can be cooled using a cooling system that circulates water throughout the inner channels of each electrode.

The film thickness was measured by Fizeau fringes method using a visible laser of 630nm wavelength to form the fringes pattern. Then, the deposition rate was determined as shown in Fig. 2. It is clear that the deposition rate is uniformly increasing for all samples, which may be attributed to the operation stability of the sputtering system. However, some slight differences can be observed due to the probability of forming more silicon nitride particles and hence increasing the film thickness.

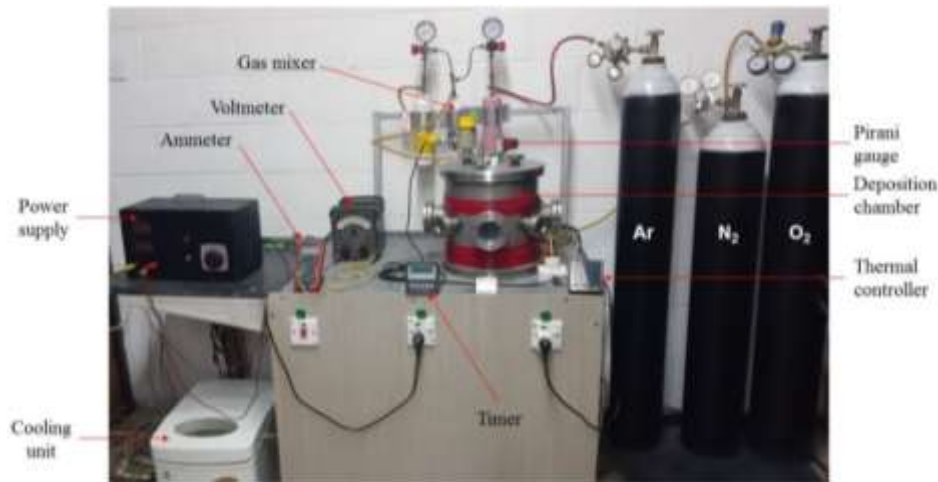


Figure 1: The DC reactive sputtering system used in this work.

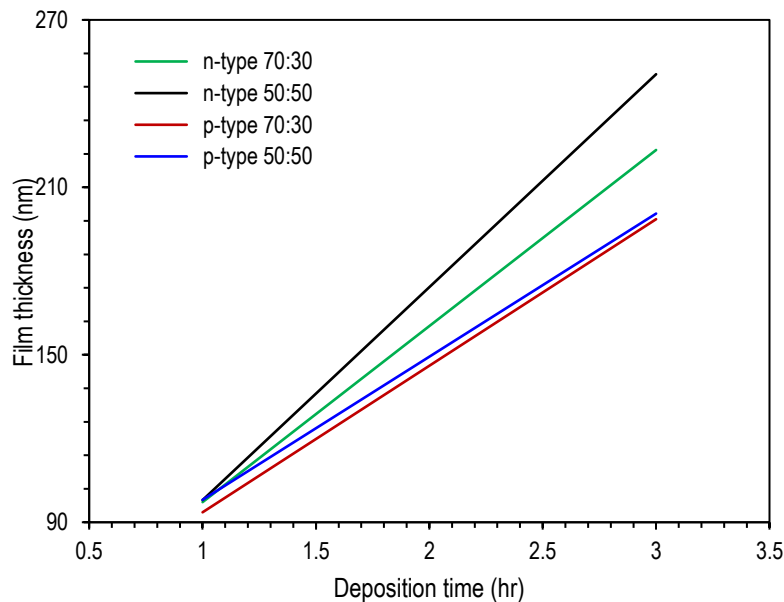


Figure 2: Deposition rates of the silicon nitride thin films prepared in this work.

The electrical conductivity of the metallic substrates was measured before and after being coated with Si_3N_4 thin films on both surfaces using a multimeter and a DC power supply in order to introduce the effect of these thin films on the electrical conductivity of these substrates.

3. Results and Discussion

To determine the optical homogeneity of the prepared thin films, the relationship between refractive index (n) (The refractive index is calculated from the reflectance of the thin film using the data of absorption measurements) and wavelength (λ) in the spectral range 400-700nm, which is known as the dispersion curve, was determined for the samples prepared using gas mixing ratio of 70:30 after different deposition times, as shown in Fig. 3. The thin films prepared from n-type silicon target showed a slight change in the refractive index value within 1.3-1.45, as shown in Fig. 3(a). This can be good indication for the optical homogeneity of these films in the visible region.

On the other hand, the thin films prepared from p-type silicon target showed relatively higher values of refractive index (1.25-1.75) and larger differences with deposition time, as shown in Fig. 3 (b).

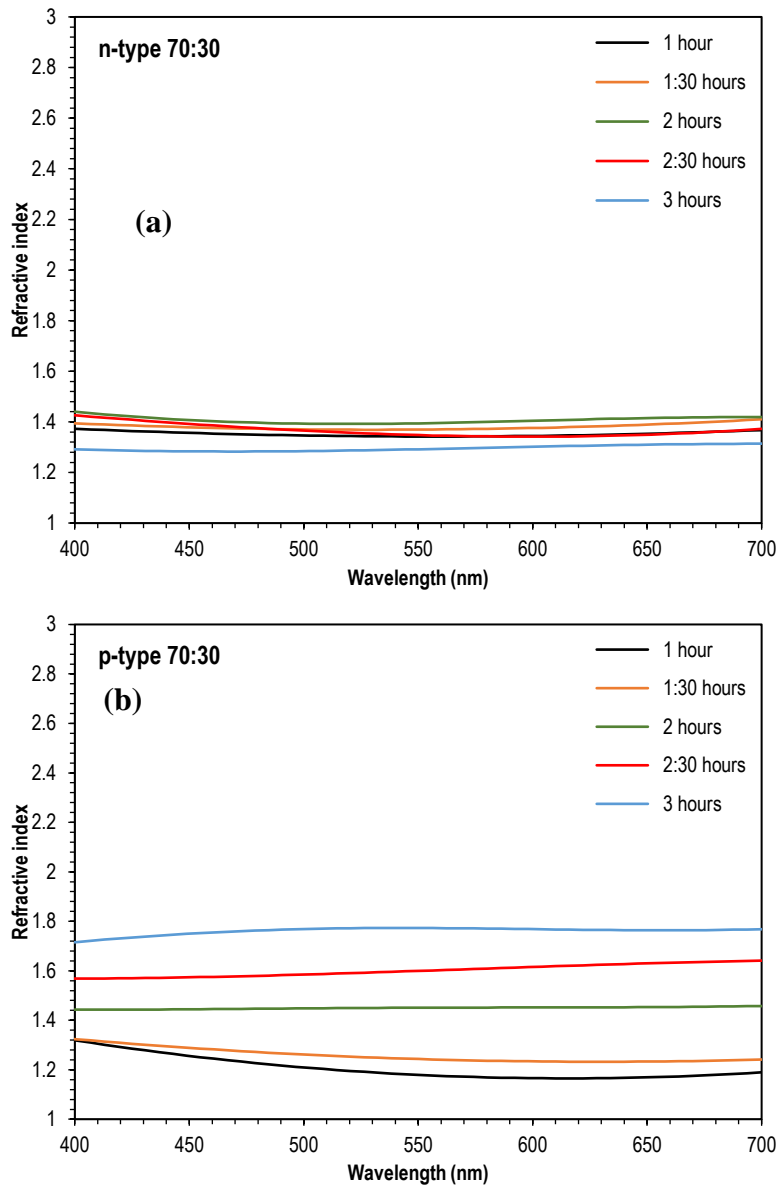


Figure 3: Dispersion curves of the silicon nitride thin film samples prepared using gas mixing ratio of 70:30 after different deposition times using both types of silicon targets using (a) n-type silicon, and (b) p-type silicon.

This may be attributed to the effect of the conductivity type of the target as the bonding configuration between silicon and nitrogen would be determined by this factor. However, all thin films prepared in this work can be described as optically homogeneous.

Fig. 4 shows the effect of type of conductivity and gas mixing ratio on the electrical conductivity of aluminum substrates coated with Si_3N_4 thin films. It is clear that the Si_3N_4 thin film prepared using a p-type Si target and gas mixture of 50:50 has caused an increase the electrical conductivity of the aluminum substrate by 1.1% while the other films have reasonably decreased the electrical conductivity of the substrate (10-40). This may be attributed to the fact that a proportion of silicon atoms bonded to nitrogen atoms keep some positive holes within the structure of the formed silicon nitride molecules as the majority carriers in p-type silicon are the positive holes [47-50]. These holes may trap electrons flowing through the thin film layers on both surfaces of the aluminum substrate and hence the recombination current may contribute to the total measured current.

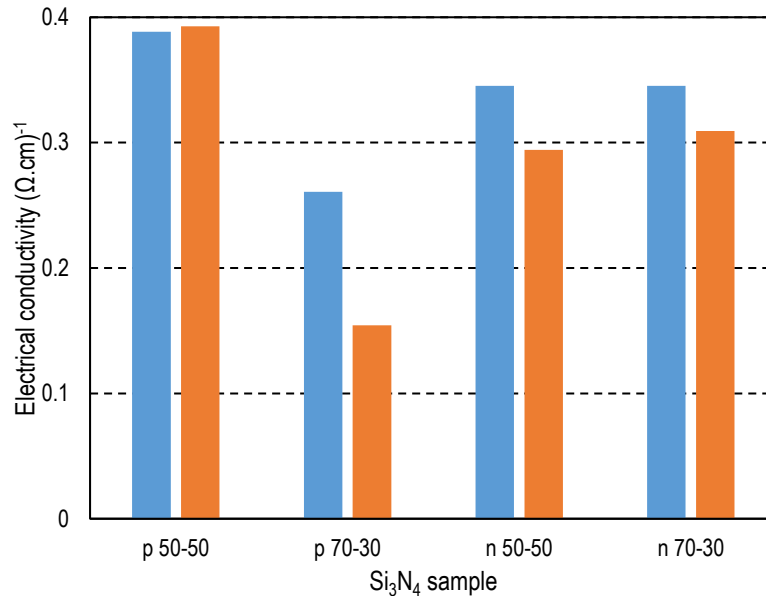


Figure 4: Effect of type of conductivity and gas mixing ratio on the electrical conductivity of aluminum substrates coated with Si_3N_4 thin films where (blue columns before coating, orange columns after coating).

On the other hand, using 70:30 gas mixture caused a reduction in the number of nitrogen atoms available for bonding with silicon atoms. Therefore, the availability of positive holes in the Si_3N_4 molecules would be higher than the previous case. Hence, trapping rate of electrons by these holes is higher and reasonably consumes these electrons with lower rate of recombination. Therefore, the total current would be lower.

In the case of Si_3N_4 thin films prepared from n-type silicon targets, in which the majority carriers are electrons, these electrons are mostly consumed in the formation of Si-N bonds, which are stronger than those in the Si_3N_4 molecules formed from p-type silicon targets. Therefore, the electrical resistance of the Si_3N_4 layer is increased due to the increase in film density. Hence, the contribution to the total current is from the electrons flowing from the DC power supply through the coated substrate. This current is certainly reduced by the electrical resistance of the Si_3N_4 films on both surfaces of the aluminum substrate.

Fig. 5 shows the effect of the type of conductivity and gas mixing ratio on the electrical conductivity of titanium substrates coated with Si_3N_4 thin films. It is clear that

the Si_3N_4 thin films prepared using both types of Si targets and both gas mixtures decreased the electrical conductivity of the titanium substrate. This may be initially attributed to the fact that titanium has lower electrical conductivity than aluminum ($\sigma_{\text{Al}} \approx 20\sigma_{\text{Ti}}$). Therefore, the ability of Si_3N_4 thin films – regardless of the conductivity type of the Si target – is sufficiently high to restrict the flow of current through the titanium substrate.

This result may be much more important than that of aluminum because titanium and its alloys are intensively used in biomedical applications such as joint replacements, dental bridges and implants, and coronary stents. Titanium is used for implants as it has low density and good mechanical properties. Titanium evokes the minimum amount of tissue reaction as it forms a tenacious oxide layer which resists further diffusion of metal ions to oxygen gas at the interface.

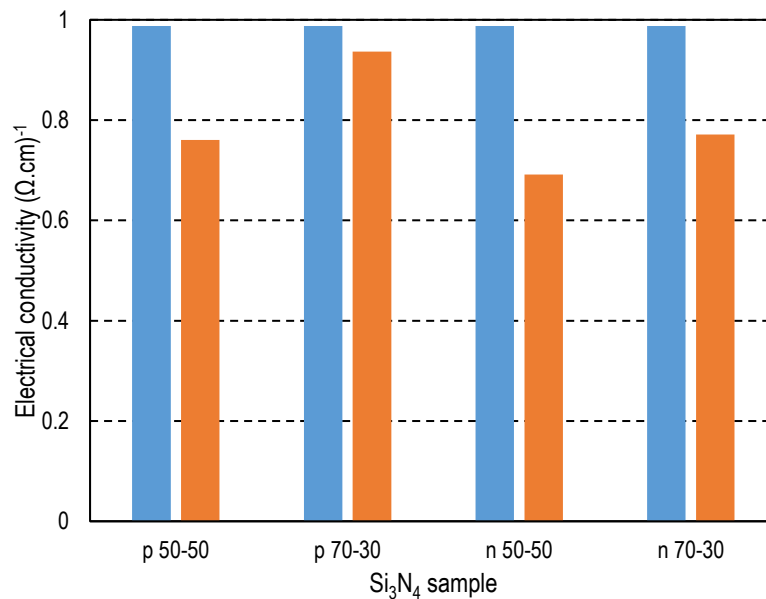


Figure 5: Effect of type of conductivity and gas mixing ratio on the electrical conductivity of titanium substrates coated with Si_3N_4 thin films were (Blue columns before coating, orange columns after coating).

4. Conclusions

In conclusion, the effects of the conductivity type of the silicon target and the Ar:N₂ gas mixing ratio used for the preparation of silicon nitride thin films by DC reactive sputtering technique have been introduced, and it has been found that the electrical conductivity of metallic substrates such as titanium can be reasonably reduced when this substrate is coated with Si_3N_4 thin films on both surfaces. This result is very important and applicable in the biomedical fields where such metals are used for joint replacements, dental bridges and implants, and coronary stents. This work represents the first attempt in Iraq to study such effects, and it may represent a good starting point for advanced studies in biomedical engineering.

Acknowledgement

Authors have acknowledged all people and institutions might submit any kind of assistance.

Conflict of interest

Authors declare that they do not have any conflict of interest related to the work included in this manuscript.

References

1. C. B. Carter and M. G. Norton. 2007, Springer: New York.
2. S. Sze, J. Appl. Phys. **38**, 2951 (1967).
3. Z. Q. Yao, P. Yang, N. Huang, J. Wang, F. Wen, and Y. Leng, Nuc. Instru. Meth. Phys. Res. Sec. B: Beam Inter. Mat. Atoms **242**, 33 (2006).
4. B. K. Nasser and M. A. Hameed, Nonlin. Opt., Quant. Opt.: Concep. Mod. Opt. **53**, 99 (2021).
5. N. Maluf, Measur. Sci. Tech. **13**, 229 (2002).
6. M. Baraheni and S. Amini, Ceram. Int. **45**, 10086 (2019).
7. T. G. Allen, J. Bullock, X. Yang, A. Javey, and S. De Wolf, Nat. Ener. **4**, 914 (2019).
8. R. B. Heimann, Materials **16**, 5142 (2023).
9. X. Du, S. S. Lee, G. Blugan, and S. J. Ferguson, Int. J. Molec. Sci. **23**, 6551 (2022).
10. P. Martin, *Introduction to surface engineering and functionally engineered materials*. (Canada, John Wiley & Sons, 2011).
11. S. V. Deshpande, E. Gulari, S. W. Brown, and S. C. Rand, J. Appl. Phys. **77**, 6534 (1995).
12. K. Prasad, O. Bazaka, M. Chua, M. Rochford, L. Fedrick, J. Spoor, R. Symes, M. Tieppo, C. Collins, and A. Cao, Materials **10**, 884 (2017).
13. J. Enderle and J. Bronzino, *Introduction to Biomedical Engineering*. 3rd Ed. (Burlington, USA, Academic Press, 2012).
14. J. Bronzino and Francis, *Medical Devices and Systems*. 3rd Ed. (Hartford, Connecticut, U.S.A, CRC Taylor, 2006).
15. G. S. Sawhney, *Fundamentals of Biomedical Engineering*. (Daryaganj, New Delhi, New Age International, 2007).
16. D. You, Y. Jiang, Y. Zhao, W. Guo, and M. Tan, Opt. Mat. **136**, 113354 (2023).
17. R. Shakoury, A. Arman, Ş. Tãlu, D. Dastan, C. Luna, and S. Rezaee, Opt. Quan. Elect. **52**, 270 (2020).
18. X. Jin, J. Kong, X. Zhou, P. Xing, and Y. Zhuang, J. Cleaner Produc. **247**, 119163 (2020).
19. T. G. Aguirre, C. L. Cramer, and D. J. Mitchell, J. Eur. Ceram. Soci. **42**, 735 (2022).
20. F. L. Riley, J. American Ceram. Soci. **83**, 245 (2000).
21. V. Pavaraarn, R. Precharyutasin, and P. Praserttham, J. American Ceram. Soci. **93**, 973 (2010).
22. A. Šaponjić, S. Ilić, T. Barudzija, A. R. Mihajlović, M. Kokunešoski, and B. Matović, J. Australian Ceram. Soci., 1 (2023).
23. Z. Gan, C. Wang, and Z. Chen, Surfaces **1**, 59 (2018).
24. N. Koosha, J. Karimi-Sabet, M. A. Moosavian, and Y. Amini, Mat. Sci. Eng.: B **274**, 115458 (2021).
25. J. Zhang, F. Wang, V. B. Shenoy, M. Tang, and J. Lou, Mat. Today **40**, 132 (2020).
26. M. Sabzi, S. Mousavi Anijdan, M. Shamsodin, M. Farzam, A. Hojjati-Najafabadi, P. Feng, N. Park, and U. Lee, Coatings **13**, 188 (2023).
27. L. M. Hoyos-Palacio, D. P. C. Castro, I. C. Ortiz-Trujillo, L. E. B. Palacio, B. J. G. Upegui, N. J. E. Mora, and J. a. C. Cornelio, J. Mat. Res. Tech. **8**, 5893 (2019).
28. K. H. Kim, K. S. Kim, Y. J. Ji, J. E. Kang, and G. Y. Yeom, Appl. Surf. Sci. **541**, 148313 (2021).
29. M. Momeni, M. Tabibiazar, S. Khorram, M. Zakerhamidi, M. Mohammadifar, H. Valizadeh, and M. Ghorbani, Int. J. Bio. Macromol. **120**, 2572 (2018).

30. M. M. Tahiyat, J. C. Stephens, V. I. Kolobov, and T. I. Farouk, J. Phys. D: Appl. Phys. **55**, 085201 (2021).
31. Y. K. Ezhovskii and S. Mikhailovskii, Russian Microelec. **48**, 229 (2019).
32. J.-M. Park, S. J. Jang, L. L. Yusup, W.-J. Lee, and S.-I. Lee, ACS App. Mat. Inter. **8**, 20865 (2016).
33. P. O. Oviroh, R. Akbarzadeh, D. Pan, R. a. M. Coetzee, and T.-C. Jen, Sci. Tech. Advan. Mat. **20**, 465 (2019).
34. O. A. Hammadi, Mat. Res. Expr. **8**, 085013 (2021).
35. A. A. Anber and F. J. Kadhim, Silicon **10**, 821 (2018).
36. B. K. Nasser and M. A. Hameed, Iraqi J. Appl. Phys. **15**, (2019).
37. A. A. Anber, O. A. Hammadi, and F. J. Kadhim, Iraqi J. Appl. Phys. **17**, (2021).
38. S. H. Faisal, Iraqi J. Appl. Phys. **16**, 27 (2020).
39. R. A. Hassan and F. T. Ibrahim, Iraqi J. Appl. Phys. **17**, 3 (2021).
40. F. J. Al-Maliki and E. A. Al-Oubidy, Phys. B: Condens Mat. **555**, 18 (2019).
41. A. M. Hameed and M. A. Hameed, Emer. Mat. **6**, 627 (2023).
42. A. Frigg, A. Boes, G. Ren, T. G. Nguyen, D.-Y. Choi, S. Gees, D. Moss, and A. Mitchell, APL Phot. **5**, 011302 (2020).
43. A. Vahl, S. Veziroglu, B. Henkel, T. Strunskus, O. Polonskyi, O. C. Aktas, and F. Faupel, Materials **12**, 2840 (2019).
44. M. Ohring, *The Materials Science of Thin Films Academic Press*. (San Diego, California, Academic Pres, 1992).
45. P. Martin. 2010, Elsevier Amsterdam.
46. O. Debieu, R. P. Nalini, J. Cardin, X. Portier, J. Perrière, and F. Gourbilleau, Nanosc. Res. Lett. **8**, 1 (2013).
47. R. Xia, Y. Zhang, Q. Zhu, J. Qian, Q. Dong, and F. Li, J. Appl. Poly. Sci. **107**, 562 (2008).
48. D. Xiang, H. Xia, W. Yang, and P. Mou, Vacuum **165**, 172 (2019).
49. F. Zhou, J. Shan, L. Cui, Y. Qi, J. Hu, Y. Zhang, and Z. Liu, Advan. Funct. Mat. **32**, 2202026 (2022).
50. I. Lisovskyy, M. Voitovych, A. Sarikov, S. Zlobin, A. Lukianov, O. Oberemok, and O. Dubikovskiy, J. Non-Crys. Sol. **617**, 122502 (2023).

توظيف أغشية نتريد السيليكون المحضرة بتقنية التبريد التفاعلي المستمر لتطبيقات الإطلاق الأيوني

ديار علي طاهر¹ و محمد عيد الله حميد¹
¹قسم الفيزياء، كلية العلوم، جامعة بغداد، بغداد، العراق

الخلاصة

في هذا البحث، جرى ترسيب أغشية رقيقة من نتريد السيليكون على قواعد معدنية (من الألمنيوم والتيتانيوم) بتقنية التبريد التفاعلي المستمر باستخدام أهداف من السيليكون المختلفة بنوع التوصيلية الكهربائية (المناحة والقبالة) وكذلك استخدام خلطتين مختلفتين لغازي الأركون والنيتروجين (50:50 و 70:30). جرى قياس التوصيلية الكهربائية للقواعد المعدنية قبل وبعد ترسيب أغشية نتريد السيليكون على كلا الجانبين. أظهرت النتائج أن الأغشية المرسبة سببت نقصاناً في التوصيلية الكهربائية للقواعد وأن أغشية نتريد السيليكون المحضرة باستخدام هدف من السيليكون المناح والخلطة الغازية 50:50 والمرسبة على جانبي قاعدة التيتانيوم قد أدت لتقليل التوصيلية الكهربائية للقاعدة بنسبة 30%. هذه النتائج تعد ذات أهمية بالغة في تطبيقات الطب الحيوي من أجل منع إطلاق الأيونات من الأجزاء المعدنية التي يتم زرعها داخل جسم الإنسان.

الكلمات المفتاحية: نتريد السيليكون، التوصيلية الكهربائية، إطلاق الأيونات، تطبيقات الطب الحيوي، تقنية التبريد التفاعلي المستمر.